06

Impact compressibility and spall strength of ultra-high molecular weight polyethylene at temperatures from -120°C to 145°C

© I.A. Cherepanov,[1] A.S. Savinykh,[1] G.V. Garkushin,[1] S.V. Razorenov,[1] A.N. Zhukov,[1] D.A. Chernyayev,[1] S.V. Panin,[2] V.O. Alexenko[2]

[1] Federal Research Center for Problems of Chemical Physics and Medical Chemistry, Russian Academy of Sciences, 142432 Chernogolovka, Moscow region, Russia
[2] Institute of Strength Physics and Materials Sciences, SB RAS, 634055 Tomsk, Russia
e-mail: i.cherepanov95@yandex.ru

Received July 2, 2025
Revised December 4, 2025
Accepted December 10, 2025

The analysis of full wave profiles for ultra-high molecular weight polyethylene samples enabled the determination of the dependences of the shock wave velocity U_S on the particle velocity u_p (Hugoniots) in the range of maximum shock compression stresses from 0.3 to 1.3 GPa at initial temperatures of -95°C to 95°C. Spall strength measurements were conducted over a broad range of initial temperatures, between -120°C to 145°C, at a maximum compression stress of 0.8 GPa. The samples were loaded by the impact of aluminium plates accelerated to velocities between 210 m/s and 660 m/s using special explosive devices or a pneumatic gun. Wave profiles were recorded using a laser Doppler velocimeter VISAR. The results demonstrate that, as observed in other polymeric materials, elevated temperatures result in a reduction in spall strength.

Keywords: UHMWPE, shock waves, deformation, temperature, spall strength, Hugoniots.

DOI: 10.61011/TP.2026.04.63266.167-25

Introduction

Increased strength, wear resistance as well as corrosion resistance make it possible to regard ultra-high-molecular-weight polyethylene (UHMWPE) as one of the best material in terms of a sum of characteristics, including for being used in space, military or medicine fields in extreme operating conditions [1–3]. Use of UHMWPE products at high strain rates in a wide temperature range creates a relevant issue about influence of the temperature on a material failure mechanism and its strength characteristics.

Primarily, UHMWPE differs from other types of polyethylene in its molecular weight (above 10^6 g/mol) [4]. Influence of an internal structure and the molecular weight on the strength characteristics was considered in the studies [5–7]. Using a molecular dynamics method, it has been demonstrated in the study [5] that dynamic tensile strength of polyethylene crystals containing short chains (120 atoms) increases in more than 7 times when the strain rate increases from 10^{10} to 10^{13} s^{-1}. The authors assume that it can be related to a change of a failure mechanism: from sliding along chain ends to direct rupture along the chain. With the increasing molecular weight, influence of the strain rate on strength occurs at its lower values. The results demonstrate that tensile strength of the polyethylene can exceed strength determined at the low strain rates. For example, using a servo-hydraulic system the study [6] has quasi-statically compressed samples of high-density polyethylene (HDPE) and UHMWPE. It was demonstrated that the HDPE sample exhibited much higher yield strength (thus, at the room temperature and the strain rate of $0.1\,s^{-1}$the value of HDPE exceeded the value for UHMWPE by 72%) due to uniform flowing. In turn, the UHMWPE samples demonstrate significant strain hardening when its yield strength is exceeded. Under dynamic loads and high values of maximum shock compression stress, there are not significant differences observed between the two types of polyethylene with the different molecular weight UHMWPE and HDPE. Data about impact compressibility of a material can be obtained based on Hugoniots, which are a set of all possible states that occur when matter is compressed by variously-intense shock waves and that can be described by a linear relationship of the kind $U_S = c_0 + bu_p$ [8] within a range of moderated compressions of media. Thus, under shock compression at pressures exceeding 33 GPa, the relationships for Hugoniots of UHMWPE and HDPE are the same within an error [7]. It was demonstrated however that under the lower pressures [9] the Hugoniots differ despite the density difference of just 3%: $U_S = 2.50 + 1.49u_p$ [km/s] for HDPE and $U_S = 2.33 + 1.56u_p$ [km/s] for UHMWPE.

Spall strength of UHMWPE was measured in the study [10]. It is demonstrated that up to a certain level it does not depend on the value of maximum shock compression stress and remains constant ~ 70 MPa, whereas when the maximum shock compression pressure exceeds 0.9 GPa, a value of spall strength decreases. The authors explain this phenomenon by two competing factors: an increase of the strain rate during tensioning and shock heating and, therefore, material softening. The same study has obtained values of the UHMWPE Hugoniot within the range up

to 2 GPa as a dependence $U_S = 2.34 + 1.895u_p$. Data about the dependence $U_S - u_p$ at the higher pressures are given in the study [7].

Usually, studies of polymer materials under dynamic loads are limited to the room temperature only. At the same time, modeling of polymer behavior in these conditions requires experimental data within a wide range of the temperatures, which also includes processes of melting and glass transition [11]. Such spall strength studies have been performed for PMMA, polycarbonate and ABS plastic [12–14]. A general trend of the studied polymer materials is expressed as reduction of the value of spall strength with the increasing temperature. If the glass transition temperature is exceeded, then depending on the internal structure this drop can be either insignificant [14] or essential and the value of spall strength approaches zero [12,13]. The present study is aimed at determining parameters of the UHMWPE Hugoniot and studying influence of the temperature on its resistance to tensile stresses (spall strength) within the range of the temperatures from $-120\,^\circ$C to $145\,^\circ$C.

1. Material and experimental setup

The experiments were done on the UHMWPE samples sintered from the GUR-2122 powder (Ticona, Germany) of the molecular weight of $4.5 \cdot 10^6$ g/mol and a particle size $5-15\,\mu$m using a hydraulic press. The samples were plates with linear sizes 40×40 mm and a thickness of 2 or 6 mm. The UHMWPE density measured by hydrostatic weighing by means of a ME204T analytical scale was $\rho_0 = 0.938\,\text{g/cm}^3$, while a longitudinal speed of sound, which is measured by means of a facility for measuring velocity of propagation of acoustic waves, (MGNIVP „Akustika“) is $c_l = (2.268 \pm 0.010)$ km/s. The DSC200L differential scanning calorimeter was used for thermal measurements of the UHMWPE samples [15]. Fig. 1 shows the DSC curve obtained at the temperature of the samples within the range $-100\,^\circ$C$-220\,^\circ$C. The heating rate V was $10\,^\circ$C/min. The curve has a thermal effect recorded and it corresponds to the melting process: $T_1 = 122\,^\circ$C is a melting start temperature, $T_2 = 150\,^\circ$C is a temperature of end of the melting process. Based on the DSC curve, we have determined sample melting enthalpy $H_m = 171$ J/g, wherein it was not possible to find the glass transition temperature T_g, which is $-160\,^\circ$C according to reference data [16]. The relationship

$$\chi_c = \frac{\Delta H_m}{\Delta H_m^0} \cdot 100\,\%$$

and enthalpy of melting of a perfect crystal $H_m^0 = 293$ J/g [17] were used to determine a crystallinity degree $\chi = 59.1\,\%$.

The crystallinity degree of the UHMWPE samples has been also determined by means of X-ray diffractometry (Fig. 2). X-ray patterns were shot in the Bragg–Brentano

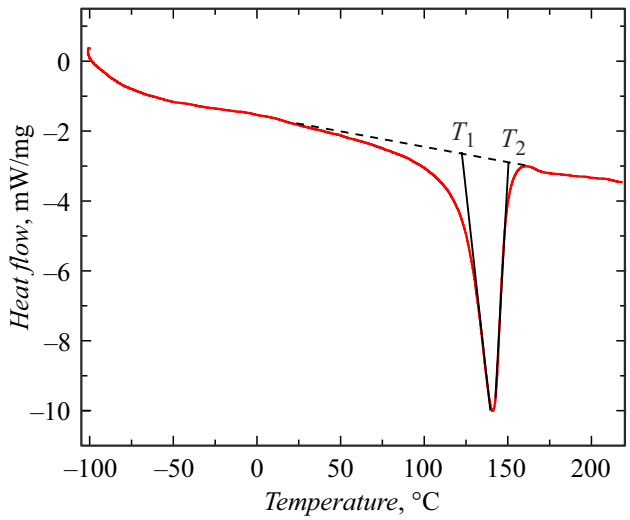

Figure 1. DSC curve of the UHMWPE sample. Heating rate $V = 10\,^\circ$C/min.

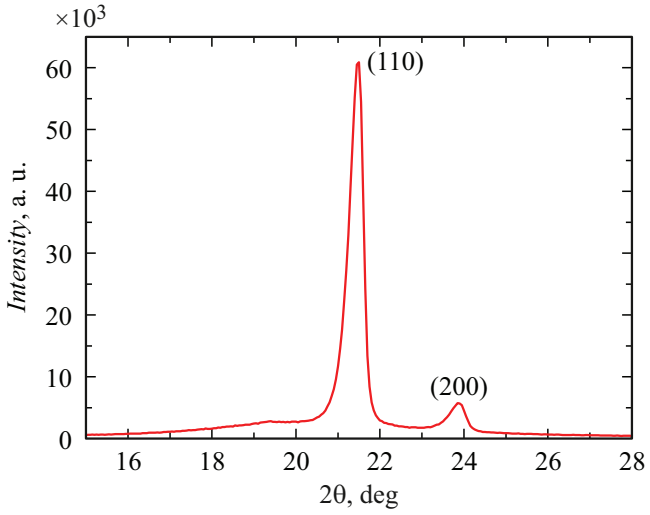

Figure 2. X-ray diffraction pattern of UHMWPE.

using the DRON-4 X-ray diffractometer and radiation was generated at a copper anode at voltage of 33 kV and current of 15 mA. A Ni filter was used to highlight the K_α line of copper. A diffraction pattern was scanned in a step-by-step mode with a step $\Delta 2\theta = 0.05^\circ$ and acquisition time $\tau = 2$ s. The UHMWPE diffraction peaks $2\theta = 21.5^\circ$ and 23.8° are caused by reflections (110) and (200) [18]. The crystallinity degree was determined as a ratio of an area of the crystalline phase peaks to a total area of the crystalline and amorphous phases [19]:

$$\chi_c = \frac{A_{cr}}{A_{cr} + A_a} \cdot 100\,\%$$

and was $\chi = 64\,\%$, thereby insignificantly differing from the result obtained by the DSC method.

The present study included three series of experiments. The first series has determined a dependence of the shock-

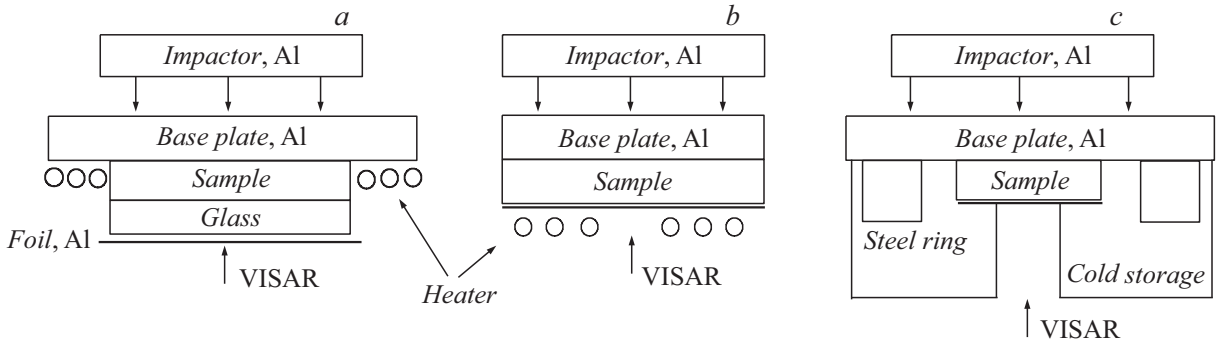

Figure 3. Diagrams of shock loading and recording of free surface velocity of the soda-lime glass (a) and the UHMWPE samples at the elevated temperatures (b) and the cryogenic (c) temperatures. a — constructing the dependences U_S-u_p; b,c — measurement of spall strength.

wave speed U_S on a particle velocity u_p (Hugoniot) within the range from $-95\,^\circ$C to $+95\,^\circ$C and at the maximum compression stresses $\sigma_{\max}$ up to 1.3 GPa. The experimental setup of the first series is shown in Fig. 3, *a*. It was loaded in a shock-wave manner by an aluminum impactor of the thickness of 7 mm, which was accelerated to the speeds (210 ± 10) m/s, (260 ± 10) m/s and (315 ± 10) m/s by means of an pneumatic barrel unit of the diameter of 50 mm. The sample was loaded through an aluminum base plate of the thickness of 4 mm, on which a composite sample was placed and it consisted of UHMWPE of the thickness of 6 mm and a soda-lime glass of the thickness of 1.2 mm. When the shock wave passes from UHMWPE into the soda-lime glass, the latter experiences maximum compression stresses $\sigma_{\max}$ that are 0.8, 1.0 and 1.3 GPa, respectively, which is significantly lower than Hugoniot elastic limit ($\sigma_{HEL} = 3.5-7$ GPa) of the glass used [20]. The experiments have recorded elastic re-reflections in the glass between a free surface of the glass and a contact surface with the UHMWPE sample. A high value of the speed of sound in the glass ($c_l = 5.720$ km/s) as compared to the studied sample makes it possible to obtain several re-reflections of the elastic wave in the glass until the reflected compression wave from the screen hits the UHMWPE–glass boundary.

The second series determined a dependence of the value of spall strength (σ_{sp}) on the maximum compression stress at the initial temperatures 20 °C and $-54\,^\circ$C. Fig. 3, *c* shows a diagram used for shock loading of the samples at the negative temperatures. A diagram shown in Fig. 3, *b* was used for measurements at the room temperature, without a heating element. The UHMWPE samples of the thickness of 2 mm were loaded by the aluminum impactors of the thickness 0.4, 0.7 and 0.9 mm and at the speeds 360 and 660 m/s. The base plate was arranged as aluminum plates of the thickness 2 or 3 mm. Detailed information about the initial parameters of the experiments as well as values of the maximum compression stress implemented in the samples are given in Table. The samples were loaded by the impactor at the speed (360 ± 10) m/s by means of the pneumatic gun, so were at the speed (660 ± 20) m/s — using explosion devices [21].

Conditions of the experiments and the results of measurements of spall strength σ_{sp} depending on the maximum compression stress $\sigma_{\max}$

№	T_0, °C	h_{bp}, mm	h_{imp}, mm	u_{imp}, m/s	$\sigma_{\max}$, GPa	$\dot{\varepsilon}_x$, 10^5 s^{-1}	σ_{sp}, MPa
1	20	1.970	0.383	360 ± 10	0.45	0.6	128
2	20	3.001	0.731	360 ± 10	0.69	1.1	130
3	20	2.998	0.734	660 ± 20	1.36	1.2	82
4	20	2.975	0.945	660 ± 20	1.57	1.5	69
5	−54	2.996	0.738	360 ± 10	0.75	0.6	148
6	−54	2.980	0.950	660 ± 20	1.44	1.7	179

Note. h_{bp} — the base plate thickness, h_{imp} — the impactor thickness, u_{imp} — the impactor speed, $\dot{\varepsilon}_x$ — the strain rate in a rarefaction wave.

The dependence of spall strength on the initial temperature of the UHMWPE samples was studied in the third series of the experiments, in which the samples of the thickness of 2 mm were loaded by the aluminum impactors of the thickness of 0.7 mm, which were accelerated to the speed of 360 m/s within the range of the initial temperatures from $-120\,^\circ$C to 145 °C.This setup was selected based on the results of the second series of the experiments.

In all the experiments, a VISAR laser Doppler velocimeter [22] with time resolution ~ 1 ns was used to record the speed of the free surface of the samples as a function of time $u_{fs}(t)$. A probing laser ray of the interferometer was reflected from an aluminum foil of the thickness of 7 μm, which was glued to the sample by a two-component epoxy glue, whose operating temperature range includes experimentally-obtained ones. The samples were heated by a ceramic heater with a nichrome spiral, which was placed on the aluminum base plate (Fig. 3, *b*). They were cooled using a chamber made of a low-porosity foam plastic, whose cavity was filled with liquid nitrogen (Fig. 3, *c*).

Long duration (15–20 min) of the cryogenic temperature was sustained using a „cold accumulator“ designed as a bulk steel ring attached to the screen. The temperature was controlled by two chromel-alumel thermocouples. One thermocouple was glued from a butt end of the sample, while the other thermocouple was glued into the sample at a distance ~ 6–7 mm from the place of recording of the free surface velocity in case of determining spall strength or into the glass–sample boundary in the series of the experiments for measuring the dependence U_S-u_p. The difference between thermocouple readings did not exceed 2 °C.Using the two thermocouples made it possible to monitor the temperature inside the sample with higher accuracy. An average sample heating rate was ~ 0.1 °C/s, while an average sample cooling rate was ~ 0.5 °C/s.

2. Measurement results

The dependences U_S-u_p were determined within the range of the initial temperatures from −95 °C to 95 °C by recording the free surface velocity profiles of the soda-lime glass glued to the UHMWPE sample of the thickness of 6.3 mm. It was loaded by the aluminum impactor of the thickness of 7 mm and a range of the impactor speeds was 210–315 m/s. Fig. 4 shows the free surface velocity profiles of the soda-lime glass at the maximum compression stress of 0.8 GPa. Recorded velocity „steps“ on the velocity profiles result from re-reflection of the elastic wave in the glass as a rarefaction wave from the free surface and a compression wave from the surface of the UHMWPE sample that has smaller dynamic impedance (a product of the density and the speed of sound).

With variation of the temperature, the elastic-wave amplitude (Fig. 4) that corresponds to a first-stage amplitude varies slightly. At the same time, measurements of the free surface velocity profiles are correct for the first two–three

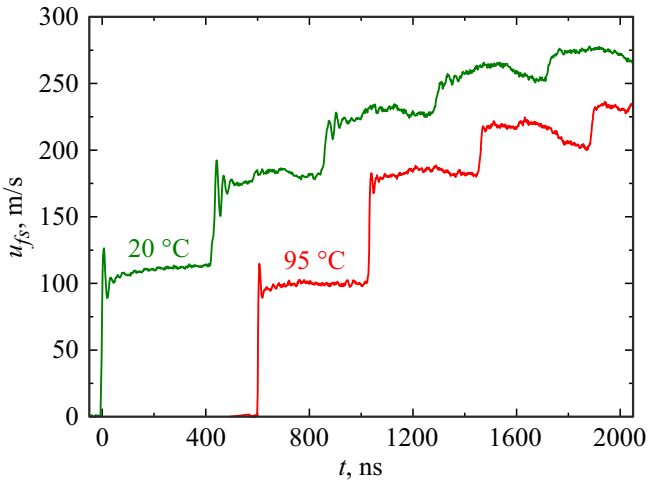

Figure 4. Free surface velocity profiles of the soda-lime glass samples loaded by the aluminum impactor of the thickness of 7 mm, accelerated to the speed of 210 m/s at 20 °C and 95 °C.

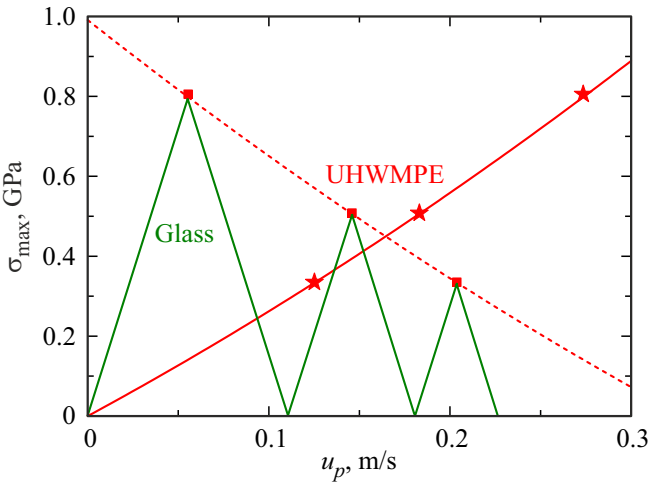

Figure 5. $\sigma_{max}-u_p$-diagram of shock-wave interactions, which is constructed from the surface speed profile at 20 °C, which is shown in Fig. 4.

steps, since subsequently the recorded surface speed are significantly distorted due to lateral unloading. A recorded time of surfacing of the next „step“ to the free surface of the glass is determined by a ratio of a double thickness of the glass to the measured longitudinal speed of sound and well agrees with one calculated for the room temperature. Within the studied temperature range, the longitudinal speed of sound of the glass varies slightly as per data of the study [23].

The values of the particle velocity and the maximum compression stress in UHMWPE during „reverberation“ of the elastic wave in the glass were found using an algorithm described in detail in the article [14]. Based on the dependences of the longitudinal speed of sound and the density of the soda-lime glass on the temperature [23–25] and the measured free surface velocity profiles, the dependences $\sigma_{max}-u_p$ have been determined by means of constructing the diagrams of shock-wave interactions (Fig. 5). The values of u_p from the measured velocity profile of the glass were taken at the first 2–3 steps that were characterized by absence of significant oscillations. The relationship $\sigma_{max} = \rho_0 U_S u_p$ was used to determined the dependence U_S-u_p.

Fig. 6 shows the obtained dependences of the shock-wave speed U_S on the particle velocity u_p for UHMWPE within the studied temperature range. The dependence is determined as $U_S = c_0 + bu_p$, where c_0 is a constant taking on a value of the bulk speed of sound, b is a coefficient to be determined from a slope of the linear dependence. With the increasing temperature, the obtained dependences U_S-u_p are lower than the Hugoniots at a lower temperature, as a result with the increasing temperature the volume speed of sound decreases. The slope of the Hugoniots characterized by the coefficient b is still almost the same at the room temperature and at the temperature of −95 °C, while at the temperature of 95 °C approaching the melting temperature

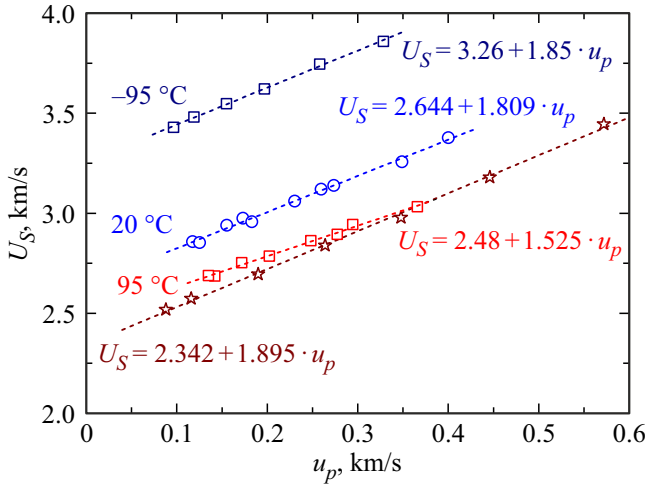

Figure 6. Results of measurements of the UHMWPE Hugoniot within the temperature range −95 °C–95 °C. An asterisk marks data of the study [10].

it decreases significantly. A difference of the value of the bulk speed of sound c_b at the room temperature from this value obtained in the study [10] can be explained by a difference in the UHMWPE samples that differ both by the crystallinity degree as well as the molecular weight. At the same time, the slope of the Hugoniots can be considered to be the same with good accuracy. It should be noted that the measured value $c_l = 2.268$ km/s in UHMWPE is significantly lower than $c_0 = 2.644$ km/s at the room temperature, therefore, no surfacing of an elastic precursor to the free surface is recorded.

Fig. 7 shows the free surface velocity profiles of the UHMWPE of the thickness of 2 mm, which are obtained at the room temperature and the temperature of −54 °C when being loaded by the aluminum impactors of the thickness 0.4, 0.7 and 0.9 mm with the speeds 360 and 660 m/s, respectively. The maximum compression stresses on the free surface, which are implemented in these experiments, have been calculated using the relationship $\sigma_{\max} = \rho_0 U_S u_p$ and did not exceed 1.6 GPa (see Table). The profiles record surfacing to the free surface for the plastic compression wave only without any signs of elastic strain. The velocity of the free surface turned out to be below the calculated one, which is related to significant decay of the shock wave when it propagates through the sample, due to catch-up by an unloading wave at the impactor side. Upon reaching the maximum velocity of the surface, output of a part of the rarefaction wave is recorded, which precedes spallation. After this, there is no spallation pulse that can be observed in other thermoplastic at the similar temperature [12,13].

The strain rate in the unloading wave was determined using the relationship $\dot{\varepsilon} = \dot{u}_{fs}/2c_b$ and the obtained values are given in Table. In the experiments performed at the same initial temperature, with the increasing maximum compression stress the strain rate in the unloading wave increases.

At the room temperature, the increase of the maximum compression stress results in reduction of a velocity decrement Δu_{fs}, which is a difference between the maximum value of the free surface velocity and the minimum one in the unloading wave, which agrees with reference data [10]. But at the temperature of −54 °C no reduction of the velocity decrement is observed. It can be explained by the fact that with temperature reduction mobility of macromolecules simultaneously decreases and significance of intermolecular forces increases. For this reason, despite the increase of the maximum compression stress resistance to tensile stresses is still at the same level.

Since the free surface velocity profiles, which are shown in Fig. 7, do not record the spallation pulses, the velocity decrement in the unloading wave was determined by variation of the slope [26]. Appearance of a fracture could be explained by a partial disruption of the material under effect of tensile stresses — a slow decrease of the velocity results from re-reflection of the rarefaction wave from a collapse surface.

The shock-wave loading was followed by examining a transect of a central part of the preserved samples in an optical microscope. The sample was cut perpendicular to an impact surface. We have not detected any assumed sign of spallation as a cavity or a group of small cavities concentrated in the same plane. Therefore, the observed fracture in the unloading wave can be explained by reduction of the speed of sound in the stretched material.

The shock-wave interactions of the impactor and the sample have been analyzed to show that a bend in the unloading wave was not caused by step-wise unloading of the impactor, since the impactor has higher dynamic impedance than the studied sample. In order to fully exclude possible recording of step-wise unloading from a stiffer impactor, an experiment has been done and it included loading by the impacted made of PMMA. The same formulation was used for an additional experiment

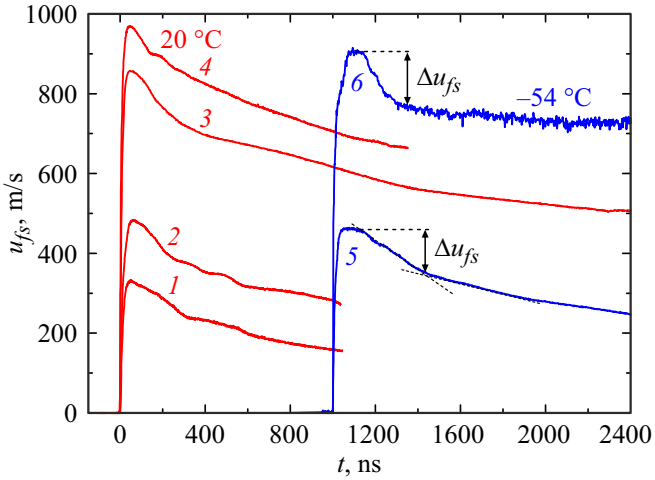

Figure 7. Free surface velocity profiles of the UHMWPE samples of the thickness of 2 mm at 20 °C and −54 °C at the various $\sigma_{\max}$. The profiles are numbered according to the Table data.

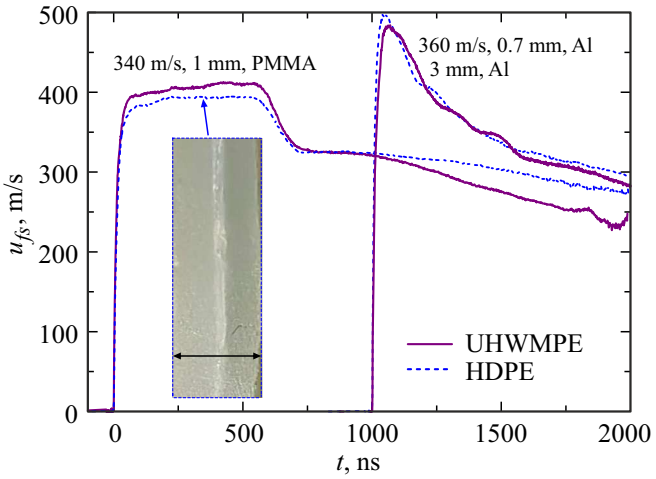

Figure 8. Free surface velocity profiles of the samples of HDPE and UHMWPE that have the thickness of 2 mm, at 20 °C.The profiles include the velocity, the thickness and the material of the impactors as well as the thickness and the material of the screen. An insert shows the transect of the central part of the preserved HDPE sample after shock-wave loading using the PMMA impactor accelerated to the speed of 340 m/s. A scale bar corresponds to 2 mm.

done with the material of a similar structure and the same composition — HDPE.

Fig. 8 shows the free surface velocity profiles of the samples of HDPE and UHMWPE, which are obtained when being loading by the PMMA impactor of the thickness of 1 mm and the aluminum impactor of the thickness of 0.7 mm with the speeds 340 and 360 m/s, respectively. When being loaded by the PMMA impactor, the spallation pulse is recorded in neither UHMWPE nor HDPE. Instead, smooth reduction of the free surface velocity is observed. When being loaded by the PMMA impactor, the speed decrement Δu_{fs} was 84 m/s in the UHMWPE experiment and 70 m/s for HDPE. When the HDPE sample is loaded by the aluminum impactor, the velocity profile similar to that in the UHMWPE experiment is qualitatively recorded. At the same time, an increase of the velocity decrement to 88 m/s is observed in the unloading wave in the HDPE experiment, so is to 103 m/s for UHMWPE. It is related to the fact that tensile stresses in the experiments reach maximum values in the sample middle when being loaded by the PMMA impactor, so are near the free surface when being loaded by the aluminum impactor [27].

Using optical microscopy of the HDPE samples, cracks were detected after loading and they were parallel to the sample plane and resulted from spallation (Fig. 8, the insert). At the same time, no sign of failure was detected in the UHMWPE samples. According to the reference data, the crystallinity degree of HDPE is 65 %–90 % [28] unlike UHMWPE having a higher portion of the amorphous part $\sim$ 40 %, which is based on pass-through chains that connect crystalline lamellas. That is why specific behavior of UHMWPE and no visible sign of spallation during shock-wave loading can be related to high-rate strain of the amorphous part of the polymer. At the same time, a detaching surface layer decelerates for a prolonged period retaining its bond with the main part of the sample. Thus, the present study addresses spall strength of UHMWPE as a magnitude characterizing nucleation of discontinuities and it also can characterize reorientation and deformation of macromolecules inside the amorphous part of the polymer in the material rather than its full disruption.

Spall strength of UHMWPE and HDPE was determined using the relationship [27]:

$$\sigma_{sp} = 1/2\rho_0 c_b \Delta u_{fs}, \qquad (1)$$

where ρ_0 is an initial density. The value of the bulk speed of sound c_b for calculating spall strength was assumed to be equal to c_0 in a dependence of the speed of the shock wave U_S on the particle velocity u_p, $U_S = c_0 + bu_p$. For UHMWPE $c_b = 2.644$ km/s, for HDPE $c_b = 2.50$ km/s, $\rho_0 = 0.961$ g/cm^3 [9]. The value of spall strength when being loaded by the impactors made of PMMA and Al was 84 and 105 MPa for HDPE and 104 and 130 MPa for UHMWPE, respectively.

Fig. 9 shows the free surface velocity profiles of the UHMWPE samples of the thickness of 2 mm, which are obtained within the range of the initial temperatures from −120 °C to 145 °C when being loaded by the aluminum impactor of their thickness of 0.7 mm that was accelerated to the speed of 360 m/s, which corresponds to $\sigma_{\max} \sim 0.7$ GPa at the room temperature. With an increase of the initial temperature of the samples the maximum values of the free surface velocity increase and significantly decrease only at the wave profiles obtained at the temperatures 134 °C and 145 °C.This change is caused by a start of the melting process at $\sim$ 122 °C, which results in changes of the internal structure of the material and origination of significant oscillations on the wave profiles.

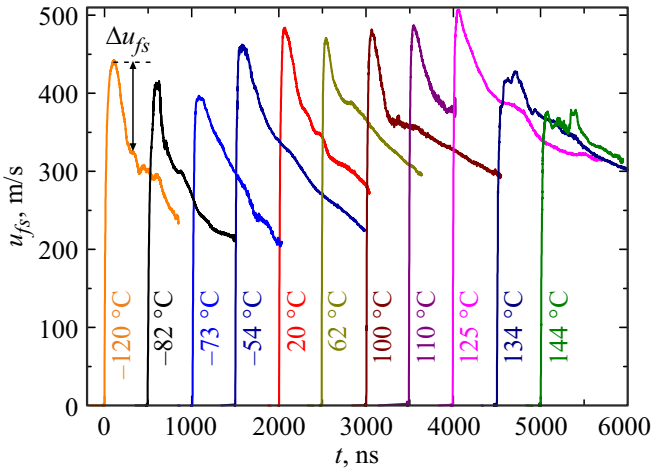

Figure 9. Free surface velocity profiles of the UHMWPE samples within the range of the temperatures from −120 °C to 145 °C.Each profile $u_{fs}(t)$ is shifted relative to the previous one by 500 ns.

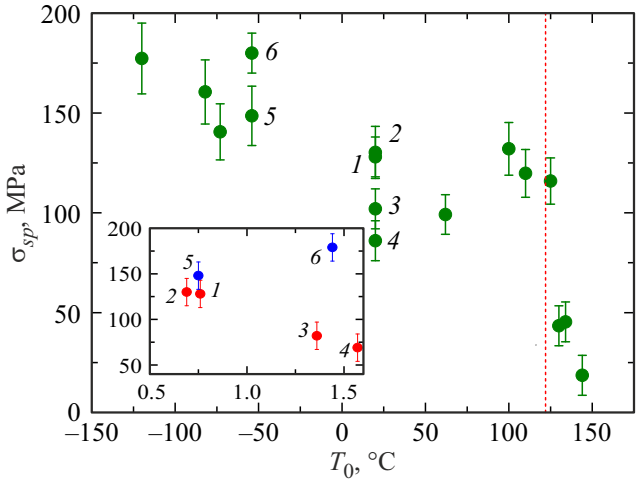

Figure 10. Dependence of spall strength of UHMWPE, which is calculated based on the wave profiles shown in Fig. 7, 9, on the initial temperature. The dashed line marks the temperature of start of the melting process. The insert shows the dependence of spall strength on the maximum compression stress. The numbers at experimental points correspond to Table.

The strain rate prior to spallation does not depend on the temperature and is within the range $0.6-1.3 \cdot 10^5\,\mathrm{s}^{-1}$.

No spallation pulse was recorded on the profiles $u_{fs}(t)$ within the entire studied temperature range. Influence of the initial temperature of the UHMWPE samples on spallation complies with collapse in other thermoplastics, such as polymethyl methacrylate and polycarbonate [12,13] in a temperature range above the glass transition temperature. A dependence of the decrement of the free surface velocity is still almost the same at the temperatures below the melting temperature and it greatly decreases when reaching it.

Spall strength was calculated based on the measured free surface velocity profiles (shown in Fig. 9) by means of the relationship (1). The bulk speed of sound c_b was determined from linear extrapolation of the dependence $c_0(T)$, which was constructed by means of values of c_0 from the dependences U_S-u_p at the initial temperatures $-95\,^\circ$C, $20\,^\circ$C and $95\,^\circ$C. The obtained value of c_0 determined in this way turned out to be higher than the measured longitudinal speed of sound at the room temperature, which does not contradict data of the study [10] and is a typical specific feature of some polymers [29]. Due to lack of reference data about the dependence $\rho(T)$ for UHMWPE and since the structure and the composition of HDPE and UHMWPE is similar, the density for each temperature was calculated based on the study [30]. A total error when determining the value of spall strength included both the above-described assumptions as well as an instrumental error when measuring the velocity decrement, which is ± 5 m/s.

Fig. 10 shows the calculated values of spall strength of UHMWPE based on the measured free surface velocity profiles, which are shown in Fig. 7, 9, using the relationship (1), within the temperature range $-120\,^\circ$C$-145\,^\circ$C.It is clear that the increase of the temperature of the samples to the melting temperature results in smooth reduction of the value of spall strength, which is related to the increase intermolecular distance as well as increased mobility of amorphous-phase macromolecules. The start of the melting process results in significant drop of all the parameters determining spall strength, which determines a nature of sharp reduction of the magnitude as a whole. At the room temperature, tensile strength of UHMWPE at static strain conditions is 43 MPa [32], which is in 2–3 times less that spall strength implemented when $\sigma_{\max} \sim 0.4-1.6$ GPa and at the respective strain rates $0.6-1.5 \cdot 10^5\,\mathrm{s}^{-1}$ obtained herein. It can be noted that as in the case of the other polymer materials UHMWPE retains a general trend of drop of spall strength with the temperature [12–14].

Conclusion

We have performed the experiments of shock-wave loading of the UHMWPE samples with an amplitude of shock compression up to 0.8 GPa within the temperature range $-120\,^\circ$C$-145\,^\circ$C and up to $\sigma_{\max} \sim 1.6$ GPa at $-54\,^\circ$C and $20\,^\circ$C with recording the free surface velocity profiles by means of the VISAR laser interferometer. We have also designed a procedure of shock-wave loading and recording of the free surface velocity profiles of the polymers at the initial temperatures that are close to the cryogenic ones. Spall strength was calculated by means of measuring UHMWPE Hugoniots at the maximum shock compression stresses of up to 1.3 GPa and within the temperature range $-95\,^\circ$C$-95\,^\circ$C. It is shown that with the increase of the temperature the bulk speed of sound (which is the first term of the linear dependence $U_S = c_0 + bu_p$) drops, while the coefficient b decreases when approaching the melting temperature. Based on analysis of the wave profiles obtained when $\sigma_{\max} \sim 0.8$ GPa, we have specified an inverse dependence of the value of spall strength on the temperature. At the same time, the dependence nature changes at the start of the melting process: smooth reduction of σ_{sp} is replaced by sharp drop in three times. Spall strength of UHMWPE is regarded as a magnitude that characterizes nucleation of discontinuities in the material rather than its full rupture. A mechanism of spallation inside the UHMWPE samples is proposed and it is based on an assumption of strain and reorientation of the pass-through chains inside the amorphous part of the polymer. With the increase of the maximum compression stress to ~ 1.6 GPa, twofold reduction of spall strength is recorded at the room temperature, whereas its slight increase is observed at the initial temperature of $-54\,^\circ$C.

Funding

The study was conduced under State Assignments of the Ministry of Education and Science of Russia

No. 124020600049-8, No. 124020800013-7 and State Assignment of Institute of Strength Physics and Materials Sciences, SB RAS, topic No. FWRW-2021-0010. The study was performed using the equipment belonging to Collective Use Center „Promising Explosion Technologies“.

Conflict of interest

The authors declare that they have no conflict of interest.

References

[1] J.H. Cha, Y. Kim, S.K.S. Kumar, C. Choi, C.G. Kim. Acta Astronautica, **168**, 182 (2020). DOI: 10.1016/j.actaastro.2019.12.008
[2] T.G. Zhang, S.S. Satapathy, L.R. Vargas-Gonzalez, S.M. Walsh. Composite Structures, **133**, 191 (2015). DOI: 10.1016/j.compstruct.2015.06.081
[3] C.A. Jacobs, C.P. Christensen, A.S. Greenwald, H. McKellop. JBJS, **89** (12), 2779 (2007). DOI: 10.2106/JBJS.G.00043
[4] J.M. Kelly. J. Macromolecular Sci., Part C, **42** (3), 355 (2002). DOI: 10.1081/MC-120006452
[5] M.A.N. Dewapriya, S.C. Chowdhury, J.M. Deitzel, J.W. Gillespie Jr. Polymer., **295**, 126779 (2024). DOI: 10.1016/j.polymer.2024.127564
[6] E.N. Brown, R.B. Willms, G.T. Gray III, P.J. Rae, C.M. Cady, K.S. Vecchio, J. Flowers, M.Y. Martinez. Experimental Mechanics, **47**, 381 (2007). DOI: 10.1007/s11340-007-9045-9
[7] D.E. Hooks, J.M. Lang, J.D. Coe, D.M. Dattelbaum. AIP Conf. Proceed., **1979**, 030004 (2018). DOI: 10.1063/1.5044774
[8] L.V. Al'tshuler. UFN, **85** (2), 199 (1965) (in Russian). DOI: 10.3367/UFNr.0085.196502a.0199
[9] D.M. Dattelbaum, B.F. Schilling, B.E. Clements, J.L. Jordan, C.F. Welch, J.A. Stull. J. Dynamic Behavior Mater., (2024). DOI: 10.1007/s40870-024-00411-3
[10] P.F. Han, D. Fan, Y. Cai, L.Z. Chen, H.L. Xie, H.W. Chai, B.X. Bie, S.N. Luo. Intern. J. Mechan. Sci., **267**, 108984 (2024). DOI: 10.1016/j.ijmecsci.2024.108984
[11] G.I. Kanel. High Temperature, **58**, 550 (2020). DOI: 10.1134/S0018151X20040057
[12] E.B. Zaretsky, G.I. Kanel. J. Appl. Phys., **126**, 085902 (2019). DOI: 10.1063/1.5116075
[13] I.A. Cherepanov, A.S. Savinykh, G.V. Garkushin, S.V. Razorenov. Tech. Phys., **68** (5), 622 (2023). DOI: 10.21883/TP.2023.05.56068.10-23
[14] I.A. Cherepanov, A.S. Savinykh, G.V. Garkushin, S.V. Razorenov. Tech. Phys., **69** (1), 119 (2024). DOI: 10.61011/JTF.2024.01.56910.247-23
[15] M.E. Brown, P.K. Gallagher. *Handbook of thermal analysis and calorimetry: recent advances, techniques and applications* (Elsevier, 2011)
[16] S.M. Kurtz. *UHMWPE biomaterials handbook* (Academic Press, 2009)
[17] S. Hu, Y. Feng, X. Yin, X. Zou, J. Qu. Polymer, **229**, 124026 (2021). DOI: 10.1016/j.polymer.2021.124026
[18] Y.L. Joo, O.H. Han, H.K. Lee, J.K. Song. Polymer, **41**, 1355 (2000). DOI: 10.1016/S0032-3861(99)00272-4
[19] L. Segal, J. Creely, A. Martin, C. Conrad. Textile Res. J., **29**, 786 (1959). DOI: 10.1177/004051755902901003
[20] G.I. Kanel, S.V. Razorenov, A.S. Savinykh, A. Rajendran, Z. Chen. AIP Conf. Proceed., **845**, 876 (2006). DOI: 10.1063/1.2263461
[21] G.I. Kanel, S.V. Razorenov, V.E. Fortov. *Shock-Wave Phenomena and the Properties of Condensed Matter* (Springer, 2004)
[22] L.M. Barker, R.E. Hollenbach. J. Appl. Phys., **43** (11), 4669 (1972). DOI: 10.1063/1.1660986
[23] A.K. Varshneya, J.C. Mauro. *Fundamentals of Inorganic glasses* (Elsevier, 2019)
[24] J.L. Jordan, D.T. Casem, J. Robinette. J. Appl. Phys., **131** (16), 165903 (2022). DOI: 10.1063/5.0082477
[25] E. Symoens, R. Van Coile, J. Belis. Glass Structures Eng., **7** (3), 457 (2022). DOI: 10.1007/s40940-022-00197-7
[26] Yu.B. Kalmykov, G.I. Kanel, I.P. Parkhomenko, A.V. Utkin, V.E. Fortov. J. Appl. Mechan. Tech. Phys., **31**, 116 (1990). DOI: 10.1007/BF00852759
[27] G.I. Kanel. J. Appl. Mechan. Tech. Phys., **42**, 358 (2001). DOI: 10.1023/A:1018804709273
[28] F.J. Stadler, T. Takahashi, K. Yonetake. e-Polymers, 40 (2009). DOI: 10.1515/epoly.2009.9.1.479
[29] R.G. McQueen, S.P. Marsh, J.W. Taylor, J.N. Fritz, W.J. Carter. In: *High velocity impact phenomena.* ed by R. Kinslow (Academic Press, NY., 1970), p. 294.
[31] K.V. Allahverdiyeva, N.T. Kakhramanov, G.S. Martynova, F.A. Mustafayeva, Y.N. Gahramanli, A.G. Habibova, R.V. Gurbanova. Heliyon, **9**, 14829 (2023). DOI: 10.1016/j.heliyon.2023.e14829 External Link
[32] S.V. Panin, L.A. Kornienko, Q. Huang, D.G. Buslovich, S.A. Bochkareva, V.O. Alexenko, I.L. Panov, F. Berto. Materials, **13** (7), 1602 (2020). DOI: 10.3390/ma13071602

Translated by M.Shevelev